TUNNEL DISPLACEMENT PREDICTION UNDER SPATIAL EFFECT BASED ON GAUSSIAN PROCESS REGRESSION OPTIMIZED BY DIFFERENTIAL EVOLUTION

S. Zheng, *A.N. Jiang*, *X.R. Yang**

Abstract: The prediction and analysis of surrounding rock deformation is a primary risk assessment method in tunnel engineering. However, the accurate prediction result is not easy to achieve due to the influence of multiple factors such as rock mass properties, support structure, and the spatial effect of tunnel construction. In this paper, a multivariate time-series model (MTSM) for tunnel displacement prediction is studied based on Gaussian process regression (GPR) optimized by differential evolutionary (DE) strategy, where the spatial effect is intuitively expressed through an extended time-series model. First, building learning samples for GPR, in which the inputs is the displacement data of the previous n days and the output is the data of the day $(n + 1)$. Then, for each sample, an input item is added successively to form an expanded learning sample, which is the "distance between the construction face and monitoring section" on the day $(n + 1)$. Taking the root mean square error between the regression and measured data as the control index, the GPR model is trained to express the nonlinear mapping relationship between input and output, and the optimal parameters of this model are searched by DE. The displacement multivariate time-series model represented by DE-GPR is known as MTSM. On this basis, the applicability of GPR for tunnel displacement prediction and the necessity of DE optimization are illustrated by comparing the prediction results of several commonly used machine learning models. At the same time, the influence of GPR and DE parameters on the regression result and the computational efficiency of the MTSM model is analyzed, the recommendation for parameter values are given considering both calculation efficiency and accuracy. This method is successfully applied to the Leshanting tunnel of Puyan expressway in Fujian province, China, and the results show that the MTSM based on DE-GPR has a good ability in the deformation prediction of the surrounding rock, which provides a new method for tunnel engineering safety control.

Key words: *displacement prediction, Gaussian process, differential evolution, spatial effect, parameter analysis*

---

*S. Zheng; A.N. Jiang – Corresponding author; X.R. Yang; Institute of Road and Bridge Engineering, Collage of Transportation Engineering, Dalian Maritime University, Dalian City, 116026, China 534821326@qq.com jiangannan@163.com yangxiurong6@163.com

1. Introduction

It is an important means to ensure construction safety by the real-time statistics and effective analysis of the rock displacement, which is an intuitive representation of tunnel stability. But the traditional displacement monitoring methods are limited by the information hysteresis and cannot effectively realize the early warning of tunnel disasters [1]. Time-series prediction is considered to be a good method to solve this problem [2,3]. This method can estimate the trend of future data according to the historical displacement, so as to realize the early warning and timely treatment of potential risks. However, it is difficult to guarantee the accuracy of the prediction results, because the historical data sequence of tunnel displacement is often shown as a complex implicit functional relationship, which is difficult to be described by the basic mathematical method [4]. Some intelligent algorithms with strong nonlinear regression ability have been applied to realize this prediction process in recent researches, such as support vector machine [5], artificial neural network [6,7], Gaussian process [8,9] and so on.

In these studies, the Gaussian process (GP) is a random method based on probability theory and mathematical statistics. The Gaussian process regression (GPR) developed from GP is a model with bayesian characteristics, which has good generalization and resolvability compared with other methods [10,12]. However, the accuracy of GPR is obviously affected by its parameters setting, and other intelligent algorithms also have similar problems. Researchers have tried various methods to optimize the parameters of the intelligent algorithm, such as particle swarm optimization (PSO) [13] differential evolution (DE) [14] bacterial foraging optimization algorithm (BFOA) [15] tabu search (TS) [16] and simulated annealing (SA) [17] et. al. In these explorations, DE considers the correlation of multiple variables on the basis of PSO, and its functional advantage has been proved in several studies [18,20]. Therefore, it will be a good solution to optimize GPR by DE.

Tunnel excavation process destroyed the original rock stress state of equilibrium, causes a redistribution of surrounding rock stress, deformation and energy. The radial constraint of the unexcavated area on the surrounding rock makes it impossible for the rock mass energy to be released completely at one time, the deformation of surrounding rock increases continuously and then tends to be stable with the advance of excavation. This kind of deformation characteristic caused by the excavation in tunnel construction is called spatial effect [21]. At present, the prediction of tunnel displacement trend is mainly discussed from the perspective of the displacement curve feature description. For example, Gao W. [22] combines grey system method and neural network to decompose the original displacement sequence into trend sequence and deviation sequence for prediction. Zheng G et al. [23] established a semi-empirical theory for predicting tunnel displacement by combining with the hardened soil model with small strain stiffness. Zhang KN et al. [24] extended the classic kriging spatial interpolation in time and space, established the prediction model of surrounding rock displacement of the tunnel by using the spatio-temporal variation function. These studies have achieved effective results, but ignore the direct cause of tunnel deformation, that is the spatial effect of excavation, and there are still the following problems. (1) These research meth-

ods are relatively complex, and there are few studies that adopt a more concise and intuitive time-series expansion method to predict the deformation of tunnel surrounding rock from the perspective of spatial effect. (2) GPR model can realize the regression analysis of displacement time-series, but its calculation accuracy is significantly affected by parameter setting. How to develop the coupling algorithm of displacement prediction with parameter optimization function still remains to be studied. (3) In the process of parameter optimization of the time-series model, the influence law of DE parameters on the optimization results is not clear.

In this paper, GPR is used to describe the variation rule of tunnel displacement, then the regression accuracy and computational efficiency of this model have been improved by the DE algorithm. Moreover, the "distance between the construction face and monitoring section" is used as a new input indicator to express the spatial effect of tunnel excavation. Based on this, a multivariate time-series model is established, namely MTSM. Furthermore, the influence of DE parameter variation on the regression effect is discussed, and the optimal value considering both computational efficiency and accuracy is presented. Finally, the MTSM method is applied to the tunnel construction of the YA15 section of the Puyan expressway, and the accuracy of this method is verified by the consistency comparison between the predicted value of surrounding rock displacement and the actual monitoring results.

2. Multivariate time-series model for tunnel

2.1 Time-series model

For tunnel engineering, the surrounding rock deformation can be predicted by the time-series model due to it is a continuous process changing along the time sequence. However, the deformation characteristic curve does not change monotonously in the construction process, which leads to the traditional time-series method can not accurately describe the complete deformation process of surrounding rock. As illustrated in Fig. 1, the surrounding rock displacement increases (section AB) with the proximity of the construction face. After the excavation of the target position, the surrounding rock displacement increases rapidly (section BC) and gradually becomes stable as the excavation surface gradually moves away (section CD). Such a change process indicates that the "distance between construction face and monitoring section" has a significant influence on the displacement of surrounding rock, which is called the spatial effect of the tunnel.

In order to reflect the influence of the spatial effect, a multivariate time-series model (MTSM) is established with the "distance from the construction surface to the monitoring section" as a new input variable, as shown in Fig. 2. For the displacement analysis of tunnel engineering, the mapping relationship in the figure is highly nonlinear and complex, it is difficult to express through curve fitting and parameter estimation. Use Gaussian process regression (GPR) to solve this problem.
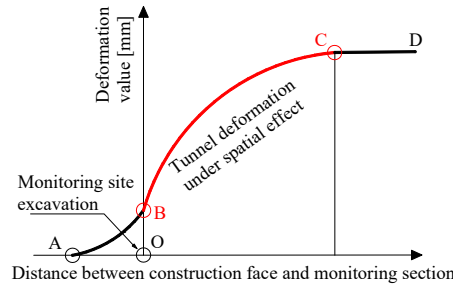
Fig. 1 *Tunnel deformation curve under the influence of spatial effect.*
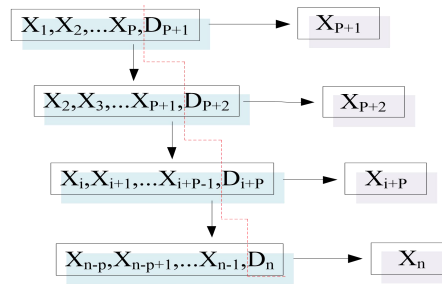

Fig. 2 *Multivariate sequentially modeling principle.*

2.2 Gaussian process regression

GPR is a probabilistic nuclear learning machine which can achieve probabilistic interpretation of the predicted output [25]. In this paper, GPR is used to establish the time-series prediction model for tunnel displacement data.

First, the learning sample is built as $D = (X, y)$, where X are the continuous displacement values for P days and the "distance between construction face and monitoring section" on day $P+1$, $X = (x_1, x_2, \ldots, x_P, D_{P+1})$, y is the displacement value on day $P+1$ at the same position. Suppose that the displacement sequence of a test point is known as (x^*, y^*), the Gaussian distribution formed by the training samples and test points is shown as formula (1).

$$\begin{bmatrix} y \\ y^* \end{bmatrix} \sim N \left(\begin{pmatrix} \mu \\ \mu^* \end{pmatrix}, \begin{bmatrix} K(X, X) + \sigma_n^2 I & K(X, x^*) \\ K(X, X)^{\mathrm{T}} & k(x^*, x^*) \end{bmatrix} \right), \tag{1}$$

where μ is the input mean of the learning sample and N stands for normal distribution. σ_n is the standard deviation of data noise, represents the fitting degree within the learning sample interval. I is a unit vector. $K(X, X)$ is the positive definite covariance matrix, representing the correlation measure of any two terms in the learning sample. For k_{ij} in the covariance matrix, the square exponential covariance function shown in formula (2) is used to solve it.

$$k_{ij}(x_i, x_j) = \sqrt{\pi} \sigma_n^2 \exp\left(-\sigma_f \|x_i - x_j\|^2\right), \tag{2}$$

where σ_f is the local correlation coefficient, representing the correlation degree between samples.

The mean value and variance of y^* can be solved as shown in formula (3) and (4), which is the solution result of tunnel displacement time-series.

$$\hat{y}\left(x^*\right) = k^{\mathrm{T}}\left(x^*\right)\left(K + \sigma_n^2 I\right)^{-1} y,\tag{3}$$

$$\hat{\sigma}^2\left(x^*\right) = k\left(x^*, x^*\right) - k^{\mathrm{T}}\left(x^*\right)\left(K + \sigma_n^2 I\right)^{-1} k\left(x^*\right).\tag{4}$$

So far, the expression and solution of MTSM by GPR have been realized. However, the local correlation coefficient σ_f and noise standard deviation σ_n in formula (2) have a significant impact on the accuracy of the model, and it is difficult to optimize these key parameters of GPR. On the one hand, multiple locally optimal solutions may occur in the process of key parameter solving. On the other hand, the regression process needs to take into account both the fitting accuracy within the learning sample interval and the extensibility of the regression model to the outside of the interval. This research solves this problem through a biological optimization strategy.

2.3   GPR optimized by DE

Differential evolution (DE) is a population-based parallel random search algorithm with real number coding. It has good robustness and simple structure, which can be solved without relying on the characteristic information of the problem. In this study, adopted the DE strategy to optimize GPR parameters as shown in Fig. 3, and the specific operation process are as follows.
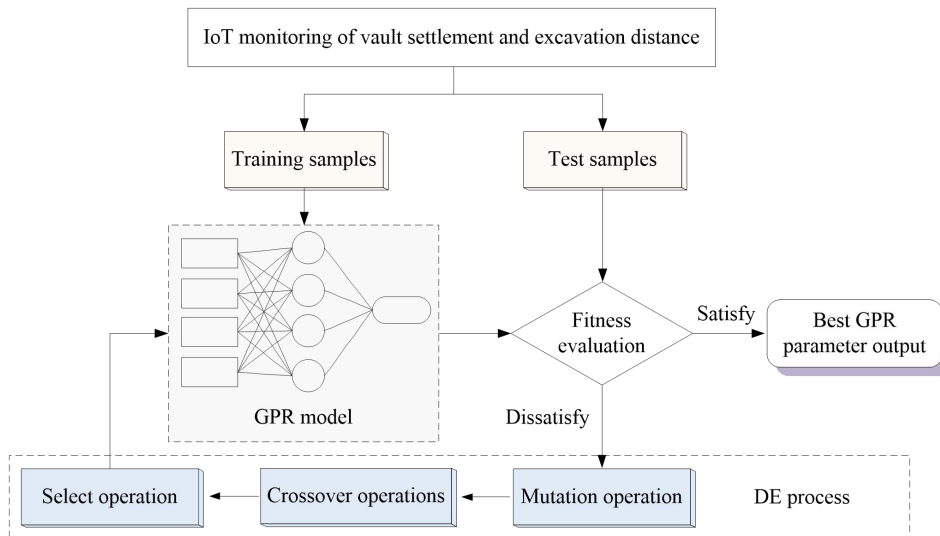

Fig. 3 *DE process to searching the optimal parameters of GPR.*

Step 1. Set the initial values of the mutation factor F and the cross factor CR of the DE algorithm, randomly generate the initial population within the parameter optimization interval.

Step 2. Based on the training samples, regression training GPR according to the key parameters in the initial population. The fitness of the regression results was evaluated with test samples. In this study, the fitness value function is the relative prediction error of the test sample group, as shown in formula (5).

$$F_{\text{it}} = \frac{\sqrt{\left[\sum_{ts=1}^{m} \left(\frac{y_{ts} - y'_{ts}}{y_{ts}} \right)^2 \right]}}{m} \tag{5}$$

where m is the number of test samples. y_{ts} and y'_{ts} are the measured value and the predicted value, respectively.

Step 3. Enter step 8 if the global minimum fitness of the current population meets the requirement, otherwise enter step 4. The fitness requirements can be set according to the calculation requirements, which is set as $\leq 10^{-2}$ in this study.

Step 4. Perform mutation operation. Generating variation vectors with two target individuals as a group, $v_i = ax_1 + bx_2$. Where a and b are randomly generated weight coefficients, $a, b \in [0, 1]$ and $a + b = 1$.

Step 5. Perform crossover operations. Cross the newly generated variation vector with the original target individual. For the optimization objective of this paper, the crossover operation is to randomly select the newly generated mutation vector and the original target individual in two dimensions to form a new vector individually.

Step 6. Perform select operation. Comparing the new individual and the original target individual, and the ones with a smaller fitness value is retained.

Step 7. Steps 4–6 are a complete DE iteration process. Determine whether the maximum number of iterations has been reached, and if so, enter step 8. Otherwise, return to step 3.

Step 8. Output the parameters represented by the individuals with the optimal fitness value, and take them as the final parameters of the GPR model to complete the optimization process.

3. Engineering application

3.1 Engineering cases

The YA15 section of Puyan expressway connects Zhongxian town to Xinkou town, Sanming city, Fujian province, China, as shown in Fig. 4. The length of this section is 9.55 km, including five tunnels, namely Jishan tunnel, Suqiao tunnel, Wugongshan tunnel, Mingxi tunnel and Leshanting tunnel respectively. The method in this paper has been applied to the prediction and early warning of tunnel deformation during the construction of this area. Take Leshanting tunnel as an example to introduce the application process of MTSM method.

The Leshanting tunnel is 601 meters in length, all of which are medium-weathered quartz-gravel. In addition to the entrance section, the tunnel is excavated by step

Fig. 4 *Tunnel engineering location and IoT monitoring system.*

method. The "distance between construction face and monitoring section" mentioned in this paper refers to the distance between the monitoring section and the upper step construction surface.

An automated Internet of Things (IoT) monitoring system has been established for some sections of the tunnel as shown in Fig. 4. The vibration wire multi-point displacement sensor is used to monitor the settlement of the tunnel vault, and the laser ranging sensor is used to monitor the distance of the tunnel face. The data obtained is processed by the YT-ZD-01 data module and then transmitted via GPRS. Such IoT monitoring overcomes the problem of insufficient manual measurement accuracy and is not affected by on-site construction factors. It can perform timing measurement at specified time intervals and obtain relatively complete isometric time-series displacement data, which provides a data basis for tunnel displacement prediction.

Practice shows that the deformation law of two adjacent tunnel monitoring sections is consistent. In order to obtain a more complete deformation prediction curve for the prediction effect analysis of the algorithm, section YK214 + 280 monitoring data in Leshanting tunnel was used to establish a learning sample for the prediction verification of the whole deformation process on section YK214 + 275.

In this process, the best historical points of surrounding rock deformation are determined as $P = 5$ through comparative analysis, that is, the input group (*input* $1 \sim 5$) is the displacement data of the measuring point for 5 consecutive days, and the output is the predicted displacement of the next day. Considering the spatial effect caused by the construction face gradually moving away from the monitoring section in tunnel construction, take the "distance between construction face and monitoring section" as an input parameter (*input6*) to construct a multivariate time-series. A total of 48 groups of learning samples were constructed, as shown in Tab. I. Among them, 8 groups of samples were randomly selected to form test samples, and the remaining 40 groups were used as training samples.

In the actual construction process, the displacement of the tunnel vault at YK214 + 280 position under the influence of space utility is mainly manifested in the first 48 construction cycles. According to this, the 48 learning samples in Tab. I are obtained. Related research [26, 27] shows that the number of samples in the machine learning process of geotechnical engineering needs to be more than 35 to

ordinal	input 1 (mm)	input 2 (mm)	input 3 (mm)	input 4 (mm)	input 5 (mm)	input 6 (m)	output (mm)
1	5.70	6.45	7.20	7.75	8.30	4.80	8.90
2	6.45	7.20	7.75	8.30	8.90	5.20	9.50
3	7.2	7.75	8.30	8.90	9.50	5.60	10.60
4	7.75	8.30	8.90	9.50	10.60	6.00	11.70
5	8.30	8.90	9.50	10.60	11.70	6.40	11.90
⋮	⋮	⋮	⋮	⋮	⋮	⋮	⋮
21	17.30	17.50	17.70	18.40	19.10	12.80	19.25
22	17.50	17.70	18.40	19.10	19.25	13.20	19.40
23	17.70	18.40	19.10	19.25	19.40	13.60	19.55
24	18.40	19.10	19.25	19.40	19.55	14.00	19.70
25	19.10	19.25	19.40	19.55	19.70	14.40	20.40
⋮	⋮	⋮	⋮	⋮	⋮	⋮	⋮
44	24.80	25.10	25.95	26.80	27.45	22.00	28.10
45	25.10	25.95	26.80	27.45	28.10	22.40	28.35
46	25.95	26.80	27.45	28.10	28.35	22.80	28.60
47	26.80	27.45	28.10	28.35	28.60	23.20	28.70
48	27.45	28.10	28.35	28.60	28.70	23.60	28.80

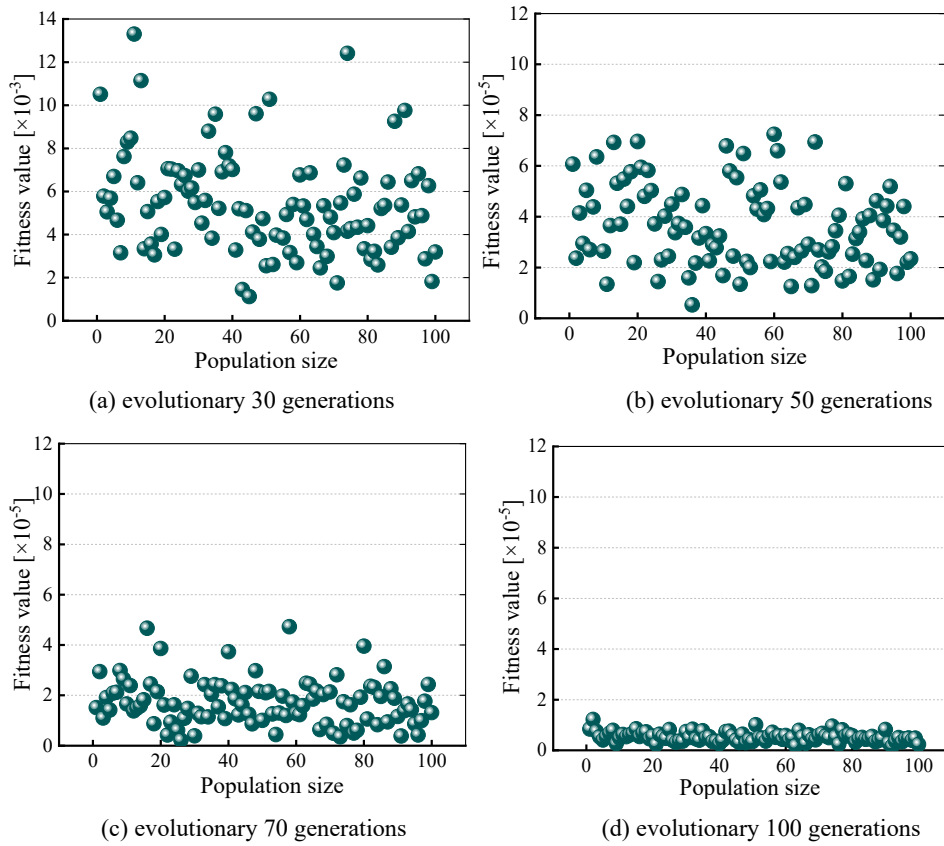**Tab. I** *Partial learning samples.*

ensure the training accuracy. The samples in Tab. I meet this requirement, but it should be noted that the expansion of learning samples will effectively improve the training effect of machine learning. Therefore, as many learning samples as possible should be collected when conditions permit. For example, when the consistency of the rock mass properties in the target area is good, it can consider comprehensively researching the data of multiple sections near the target to construct learning samples.

3.2 Prediction result analysis

The DE-GPR model described in Chapter 2 is programmed on the MATLAB platform, and after training it with the learning samples in Tab. I, the time-series prediction of the vault displacement on the YK214 + 275 segment is carried out. During the process of DE optimizing GPR key parameters, the adaptive values of the populations in the 30th, 50th, 70th and 100th generation are shown in Fig. 5. The final key parameters optimization results are $\sigma_f = 1.74$ and $\sigma_n = 0.46$.

Fig. 6 shows the displacement prediction results and their relative error statistics. It can be found that the MTSM method is basically consistent with the traditional time-series in the initial stage of the prediction process. With the increase of rolling times, the prediction curve of the ordinary time-series model approximately presents a straight line, and the error accumulation is obvious. The predicted results of MTSM are in good agreement with the measured displacement curve, with

(a) evolutionary 30 generations

(b) evolutionary 50 generations

(c) evolutionary 70 generations

(d) evolutionary 100 generations

Fig. 5 *Individual fitness value distribution in the iterative process of DE-GPR.*

the maximum absolute error of 0.65 mm and the relative error of 3.45 % in the overall prediction process.

Under the action of spatial effect, the deformation rate of surrounding rock gradually decreases and finally tends to be stable. It is difficult for the traditional time-series to obtain the change process of deformation rate through simple regression of displacement data. Therefore, in the late stage of rolling prediction, the deformation prediction curve shows a continuous rise of nearly equal rate.

For the MTSM established in this paper, the new input item "distance between construction face and monitoring section" enables the machine learning model to understand the spatial effect interval more accurately. The nonlinear mapping model established by MTSM is no longer a simple displacement data, but contains a relatively independent reference term, effectively characterizing the deformation rate of the surrounding rock under different excavation footage under the action of spatial effect. Therefore, MTSM can effectively identify the real deformation process and predict the displacement curve closer to the actual situation.
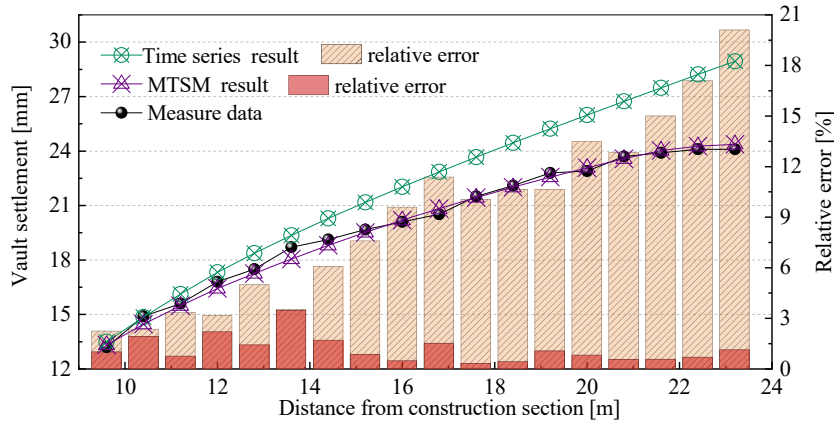
Fig. 6 *Time-series prediction results contrast.*

3.3 Discussion

The above research proves that the multivariate time-series model (MTSM) established in this paper can accurately describe the deformation process of the spatial tunnel effect. Based on this, the performance of the DE-GPR algorithm used in the research process is further verified in this section.

3.3.1 Impact of historical data volume

Adjust the learning samples and set the number of historical data in MTSM as $2 \sim 6$, respectively, the calculated error statistics of the prediction results are shown in Fig. 7. It can be seen that when the amount of historical data used exceeds 4 days, the calculation error is significantly reduced, and the predicted results are in good agreement with the actual results. When the historical data rises from 5 days to 6 days, the error changes are not obvious. Therefore, the historical data input volume is selected as 5 days in this study.
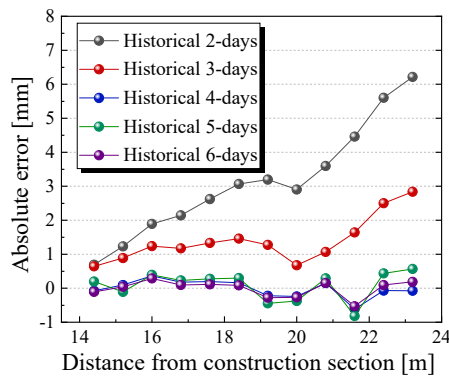

Fig. 7 *Comparison of the number of historical data input.*

3.3.2 Necessity of GPR optimization

Adjusting the values of hyperparameters σ_f and σ_n of the GPR model, the calculated regression error is shown in Fig. 8. It can be seen that the relative error distribution of the predicted results presents an irregular surface under different key parameters combination conditions. The results show that the two key parameters have a significant influence on the calculation accuracy of GPR, which proved that it is necessary to optimize these two parameters by DE.
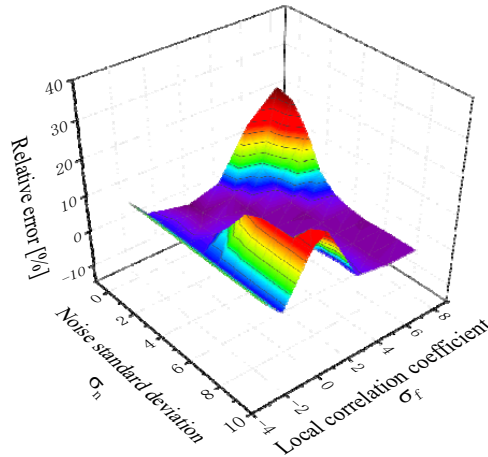

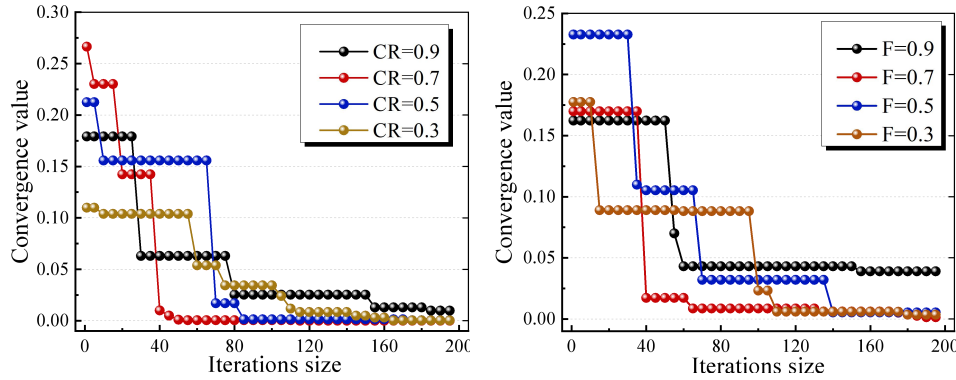**Fig. 8** *Key parameters sensitivity analysis of GPR.*

3.3.3 DE parameter selection

In order to obtain better calculation results, the key parameter settings of DE are compared. Control the variation factor F and cross factor CR as a single variable respectively, the influence of these two parameters on DE algorithm is analyzed according to the recorded convergence curve of the iterative process.

First, based on the relevant research experience of DE strategy [28], fixed F as 0.6, and CR is $0.3 \sim 0.9$ in turn. As shown in Fig. 9, the convergence effect of the iterative convergence curve is the best when $CR = 0.7$. The value of F at this time is determined based on experience, because the law of convergence characteristics with the change of CR value under different F value conditions is consistent, so this approach can effectively obtain the optimal CR value [29, 31].

Then, CR was fixed as 0.7, and F was valued from 0.3 to 0.9, respectively. F represents the single search shrinkage range. As shown by the curve on the right of Fig. 9, the convergence effect was best when $F = 0.7$.
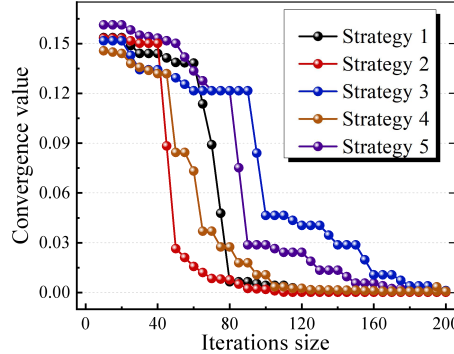
Keeping CR = 0.7 and F = 0.7 unchanged, using different DE evolution strategies in formula (6) to optimize the parameters of GPR, among them, ν_i is the vector after mutation. x_{best} is the individual with the smallest fitness value in the current population. $x_{r1} \sim x_{r4}$ are the random vectors in the process of DE. The

Fig. 9 *The iterative convergence curves under a variety of FCR value changed conditions.*

convergence curve is shown in Fig. 10, it can be seen that the convergence effect is best when strategy 2 is adopted.

$$
\begin{cases}
\text{Evolution strategy } 1 : \nu_i = x_{r1} + F(x_{r2} - x_{r3}) \\
\text{Evolution strategy } 2 : \nu_i = x_{\text{best}} + F(x_{r2} - x_{r3}) \\
\text{Evolution strategy } 3 : \nu_i = x_{r1} + F(x_{r2} - x_{r3} + x_{r4} - x_{r5}) \\
\text{Evolution strategy } 4 : \nu_i = x_{\text{best}} + F(x_{r1} - x_{r2} + x_{r3} - x_{r4}) \\
\text{Evolution strategy } 5 : \nu_i = x_{r1} + F(x_{\text{best}} - x_{r2} + x_{r3} - x_{r4})
\end{cases}
\quad . \quad (6)
$$

Fig. 10 *Impact of evolutionary strategy on convergence.*

3.3.4   GPR performance verification

According to the learning samples in Tab. I, three methods: artificial neural network (ANN), support vector machine (SVM) and Gaussian process regression (GPR) are used to predict the tunnel displacement at YK214 + 275, the prediction curves are shown in Fig. 11. In this process, SVM uses the least squares value function, and its kernel function is selected as the radial basis function:
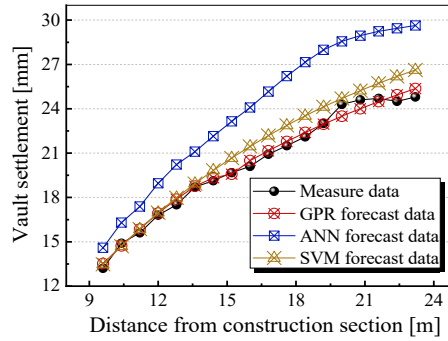
Fig. 11 *Comparative validation of different algorithms.*

$K(x, x_k) = \exp(-\|x - x_k\|^2 / \sigma^2)$, the kernel parameter setting of the algorithm obtained by the conjugate gradient method are set as: $\gamma = 6.39 \sigma^2 = 1.13$. ANN uses a BP feed-forward neural network with a hidden layer of 1, in which the number of hidden layer nodes $N_f = 5$, the number of iterations $E_p = 100$, and the learning rate $L_r = 0.1$.

It can be seen that compared with other machine learning methods (taking ANN and SVM as examples), the prediction curve of GPR is closer to the actual measurement results, indicating that GPR has better applicability in the prediction of time-series of surrounding rock displacement.

3.3.5 DE performance verification

In order to verify the performance of the DE-GPR algorithm established in this paper, a performance evaluation index R^2 is used to evaluate the predictive effect of GPR and DE-GPR, respectively, as shown in formula Eq. (7).
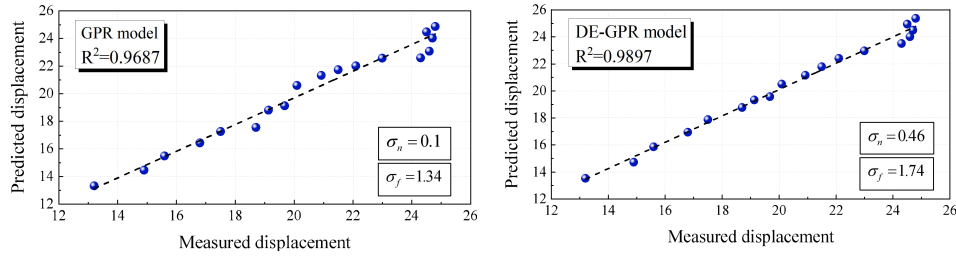
$$R^2 = \frac{[\sum_{i=1}^{n} (x_i - x_{\text{mean}})^2] - [\sum_{i=1}^{n} (x_i - x_{ip})^2]}{[\sum_{i=1}^{n} (x_i - x_{\text{mean}})^2]}, \tag{7}$$

where x_i is the measured value and x_{ip} is the corresponding predicted value. x_{mean} is the average value of the measurement.

Fig. 12 shows the R^2 evaluation of the predicted results of these two models. It can be seen that the key parameter value of GPR changed after DE optimization, and the predicted result ($R^2 = 0.9897$) of DE-GPR is significantly improved compared with the predicted result ($R^2 = 0.9687$) of GPR, indicating that the GPR model after DE optimization has a better computational performance.

4. Conclusion

In this paper, the DE-GPR model is used to express the time-series of surrounding rock deformation, and an MTSM method is established to improve the accuracy of tunnel displacement prediction. This method was applied to the construction of Leshanting tunnel, and the following conclusions were obtained.

Fig. 12 R^2 *evaluation of the predicted results of the GPR and DE-GPR model.*

(1) The two key parameters of local correlation coefficient σ_f and noise standard deviation σ_n of GPR have a significant influence on the regression prediction results, so it is necessary to select the appropriate parameters when using GPR for data mapping.

(2) In the application process, in order to obtain a better optimization effect, the initial parameters of DE are recommended to be set as: variation factor F = 0.7 and cross factor CR = 0.7.

(3) Comparative analysis shows that GPR has better applicability to tunnel displacement prediction than other intelligent algorithms. The predictive ability of GPR after DE optimization is significantly improved. The evaluation coefficient R^2 increased from 0.9687 to 0.9897, indicating that the DE-GPR model established in this paper is effective.

It should be noted that this study mainly considers the influence of spatial effects in the process of tunnel excavation. At this time, accurate measurement of the "distance between construction face and monitoring section" is necessary. Therefore, this method is mainly suitable for tunnels excavated by the full-section or step method, and the IoT monitoring system described in the article is also designed for this kind of tunnel. For other types of tunnels, it can refer to the extended time-series method of this study, but the existing models are difficult to directly apply. For example, for shield tunnels, the influence of the supporting force of the tunnel face on the tunnel deformation should be mainly considered; for tunnels excavated in blocks using the double-side heading method, the center diaphragm method, etc., the transition logic of the construction steps should be focused on.

Acknowledgement

References

[1] YANG G.B., ZHANG C.P., CAI Y. Complex analysis of ground deformation and stress for a shallow circular tunnel with a cavern in the strata considering the gravity condition. KSCE Journal of Civil Engineering, 23, 9, 2019, pp. 4141–4153.

[2] ZHU X., XU Q., TANG M.G. A hybrid machine learning and computing model for forecasting displacement of multifactor-induced landslides. Neural Computing & Applications, 30, 12, 2018, pp. 3825–3835.

[3] WANG Y.K., TANG H.M., WEN T. A hybrid intelligent approach for constructing landslide displacement prediction intervals. Applied Soft Computing, 81, 2019, pp. 1–16.

[4] ZHAO Q., MA G.Y., WANG Q. Generation of long-term In SAR ground displacement time-series through a novel multi-sensor data merging technique: The case study of the Shanghai coastal area. ISPRS Journal of Photogrammetry and Remote Sensing, 154, 2019, pp. 10–27.

[5] WEN T., TANG H.M., WANG Y.K. Landslide displacement prediction using the GA-LSSVM model and time series analysis: a case study of Three Gorges Reservoir, China. Natural Hazards and Earth System Sciences, 17, 12, 2017, pp. 2181–2198.

[6] ZHANG Y., WANG X.P., TANG H.M. An improved Elman neural network with piecewise weighted gradient for time series prediction. Neurocomputing, 359, 2019, pp. 199–208.

[7] ZHANG Y.Z. Application of improved BP neural network based on e-commerce supply chain network data in the forecast of aquatic product export volume. Cognitive Systems Research, 57, 2019, pp. 228–235.

[8] HU B., SU G.S., JIANG J.Q. Uncertain prediction for slope displacement time-series using Gaussian process machine learning. IEEE Access, 7, 2019, pp. 27535–27546.

[9] MA Z.Y., ZHANG W., LUO Z.B. Ultrasonic characterization of thermal barrier coatings porosity through BP neural network optimizing Gaussian process regression algorithm. Ultrasonics, 100, 2019, 105981.

[10] ZHU B., PEI F.H., YANG Q. Gaussian process regression-based response surface method and reliability analysis of slopes. Chinese Journal of Geotechnical Engineering, 41, S1, 2019, pp. 209–212.

[11] FANG Y., LIU B.G. Elasto-plastic parameter inversion of tunnel engineering based on genetic-Gaussian process regression algorithm. Chinese Journal of Geotechnical Engineering, 33, 6, 2011, pp. 883–889.

[12] SU G.S., ZHAO W., PENG L.F., YAN L.B. Gaussian process-based dynamic response surface method for estimating slope failure probability. Rock and Soil Mechanics, 35, 12, 2014, pp. 3592–3601.

[13] LIU W., GUO G., CHEN F.J. Meteorological pattern analysis assisted daily PM2.5 grades prediction using SVM optimized by PSO algorithm. Atmospheric Pollution Research, 10, 5, 2019, pp. 1482–1491.

[14] LI Z., XIA Y., JI Z.X. Brain voxel classification in magnetic resonance images using niche differential evolution based Bayesian inference of variational mixture of Gaussian. Neurocomputing, 269, S1, 2017, pp. 47–57.

[15] ZENG Z.G., GUAN L.H., ZHU W.Q. Face recognition based on SVM optimized by the improved bacterial foraging optimization algorithm. International Journal of Pattern Recognition and Artificial Intelligence, 33, 7, 2019, 1956007.

[16] LI Y.C., LIAN S.D. Improved fruit fly optimization algorithm incorporating tabu search for optimizing the selection of elements in trusses. KSCE Journal of Civil Engineering, 23, 6, 2018, pp. 4940–4954.

[17] FENG Y.G. Compatible topologies and parameters for NMR structure determination of carbohydrates by simulated annealing, Plos One, 12, 12, 2017, e0189700.

[18] ZHAO T.F., LIU L.F., LIU L. Differential evolution particle filtering channel estimation for non-line-of-sight wireless ultraviolet communication. Optics Communications, 451, 2019, pp. 80–85.

[19] VALI M.H., AGHAGOLZADEH A., BALEGHI Y. Optimized watermarking technique using self-adaptive differential evolution based on redundant discrete wavelet transform and singular value decomposition. Expert Systems with Applications, 114, 2018, pp. 296–312.

[20] BAIG M.Z., ASLAM N., SHUM H. Differential evolution algorithm as a tool for optimal feature subset selection in motor imagery EEG. Expert Systems with Applications, 90, 2017, pp. 184–195.

[21] ZHAO D.P., JIA L.L., WANG M.N., WANG F. Displacement prediction of tunnels based on a generalised Kelvin constitutive model and its application in a subsea tunnel. Tunnelling and Underground Space Technology, 36, 54, 2016, pp. 29–36.

[22] GAO W. Integrated intelligent method for displacement prediction in underground engineering. Neural Processing Letters, 47, 3, 2018, pp. 1055–1075.

[23] ZHENG G., YANG X.Y., ZHOU H.Z., DU Y.M., SUN J.Y., YU X.X. A simplified prediction method for evaluating tunnel displacement induced by laterally adjacent excavations. Computers and Geotechnics, 95, 2018, pp. 119–128.

[24] ZHANG K.N., HU D., HE J., WU Y.P. Tunnel construction of dynamic displacement prediction based on unified space-time Kriging model. Journal of Central South University of Science and Technology, 48, 12, 2017, pp. 3328–3334.

[25] RASMUSSEN C.E., WILLIAMS C.K.I. Gaussian processes for machine learning. Massachusetts: MIT Press, 2006.

[26] LIU K., LIU B., FANG Y. An intelligent model based on statistical learning theory for engineering rock mass classification. Bulletin of Engineering Geology and the Environment, 78, 6, 2018, pp. 4533–4548.

[27] LI S.C., HE P., LI L.P., SHI S.S., ZHANG Q.Q., ZHANG J., HU J. Gaussian process model of water inflow prediction in tunnel construction and its engineering applications. Tunnelling and Underground Space Technology, 69, 2017, pp. 155–161.

[28] FAN D., LEE J. A hybrid mechanism of particle swarm optimization and differential evolution algorithms based on Spark. KSII Transactions on Internet and Information Systems, 13, 12, 2019, pp. 5972–5989.

[29] ZHAO F., XUE F., ZHANG Y., Ma W.M., Zhang C., Song H.B. A hybrid algorithm based on self-adaptive gravitational search algorithm and differential evolution. Expert Systems with Applications, 113, 2018, pp. 515–530.

[30] DUONG N., HIEN T., HIEU N., HOANG N.D. A success history-based adaptive differential evolution optimized support vector regression for estimating plastic viscosity of fresh concrete. Engineering with Computers, 37, 2, 2021, pp. 1485–1498.

[31] VALI M.H., AGHAGOLZADEH A., BALEGHI Y. Optimized watermarking technique using self-adaptive differential evolution based on redundant discrete wavelet transform and singular value decomposition. Expert Systems with Applications, 114, 2018, pp. 296–312.